International Journal of Mechanical, Industrial and Aerospace Sciences
ISSN: 2517-9950
Vol:11, No:9, 2017

Numerical Investigation of Multiphase Flow in Pipelines

Gozel Judakova, Markus Bause

Abstract—We present and analyze reliable numerical techniques for simulating complex flow and transport phenomena related to natural gas transportation in pipelines. Such kind of problems are of high interest in the field of petroleum and environmental engineering. Modeling and understanding natural gas flow and transformation processes during transportation is important for the sake of physical realism and the design and operation of pipeline systems. In our approach a two fluid flow model based on a system of coupled hyperbolic conservation laws is considered for describing natural gas flow undergoing hydratization. The accurate numerical approximation of two-phase gas flow remains subject of strong interest in the scientific community. Such hyperbolic problems are characterized by solutions with steep gradients or discontinuities, and their approximation by standard finite element techniques typically gives rise to spurious oscillations and numerical artefacts. Recently, stabilized and discontinuous Galerkin finite element techniques have attracted researchers' interest. They are highly adapted to the hyperbolic nature of our two-phase flow model. In the presentation a streamline upwind Petrov-Galerkin approach and a discontinuous Galerkin finite element method for the numerical approximation of our flow model of two coupled systems of Euler equations are presented. Then the efficiency and reliability of stabilized continuous and discontinous finite element methods for the approximation is carefully analyzed and the potential of the either classes of numerical schemes is investigated. In particular, standard benchmark problems of two-phase flow like the shock tube problem are used for the comparative numerical study.

Keywords—Discontinuous Galerkin method, Euler system, inviscid two-fluid model, streamline upwind Petrov-Galerkin method, two-phase flow.

I. Introduction

THE increase of natural gas applications, consumption and gas infrastructure are constantly at stake. Roughly speaking, natural gas infrastructure consists of gas exploration followed by field development and finally its transportation. The latter corresponds to the transfer of natural gas through the available pipeline network. During this transport phase several problems arise making it a bottleneck in the energy supply network, thus affecting its development and operation. Therefore, optimal transfer of natural gas plays a significantly important role not only in the whole energy supply chain but also for the environment protection.

The main issue that arises when transporting natural gas through the pipeline network is the existence of an unbalanced flow rate at the start and at the end of the selected pipelines. This value oscillates between 1 % and 3 % of the total volume of transferred gas in "provider-consumer" system [1]. For simplicity and without loss of generality, in this work we will focus on the differences of flow rates in a single linear pipeline section. It is important to remark that our study can be therefore eventually extended to the whole pipeline network as well.

M. Bause, G. Judakova Department of Mechanical Engineering, Helmut Schmidt University, Holstenhofweg 85, 22043 Hamburg, Germany (phone: +49 40 6541-2721; e-mail: bause@hsu-hh.de, gjudakova@hsu-hh.de).

Flows that contain matter in different states are known as multiphase flows. For our application the compressible flow becomes a two-phase flow: the gas-liquid and the particle laden gas flow. In the study of such kind of flows, the structure of the mathematical models vary depending on a priori assumptions made regarding the design of the pipeline network and its operation. The basic model for inviscid gas flow is the Euler equation, which is an active field of research from the mathematical and numerical point of view. In particular, the numerical simulation of gas dynamics problems have gained great interest, specially from the industry sector. Starting from the two-fluid model for two-phase flows, finite element schemes with continuous and discontinuous element types and stabilization techniques are under investigation.

II. Mathematical Modeling

Let us consider the mathematical model of a two-phase flow in a pipeline. To obtain the mathematical model of the two-phase flow we follow the method and the assumptions proposed by Drew and Passman [2] and by Ishii [3] for incompressible two-phase flows and apply these principles to compressible flows. In each phase of our two-phase flow problem we use the single-phase hyperbolic conservation laws, because the viscosity and heat conduction of gases are rather small [4].

We consider a hyperbolic two-phase flow model for nonhomogeneous, nonequilibrium two-phase flow conditions, which is based on the two-fluid model. Using the balance equations for mass, momentum, and energy for each phases k (gas phase: $k = g$ and liquid phase: $k = l$ or solid phase: $k = s$), we have that

$$\begin{aligned} \frac{\partial(\rho_k)}{\partial t} + \bigtriangledown\cdot(\rho_k \boldsymbol{v}_k) &= \sigma_k^{\Gamma}, \\ \frac{\partial(\rho_k \boldsymbol{v}_k)}{\partial t} + \bigtriangledown\cdot(\rho_k \boldsymbol{v}_k \otimes \boldsymbol{v}_k) + \bigtriangledown p_k &= \boldsymbol{\sigma}_k^{\boldsymbol{F}}, \\ \frac{\partial(E_k)}{\partial t} + \bigtriangledown\cdot((E_k + p_k)\boldsymbol{v}_k) &= \sigma_k^{Q}, \end{aligned} \tag{1}$$

where, the source terms σ_k^{Γ}, $\boldsymbol{\sigma}_k^{\boldsymbol{F}}$, σ_k^{Q} are the interfacial mass, momentum and energy transfer for each of the phases, respectively. The interfacial mass transfer for each phases is defined as

$$\sigma_k^{\Gamma} = \begin{cases} -\Gamma, & k = g, \\ \Gamma, & k = l, s, \end{cases}$$

where the source term Γ is the interfacial mass exchange between the phases.

The interfacial momentum transfer for each phases is expressed as

$$\boldsymbol{\sigma}_k^{\boldsymbol{F}} = \begin{cases} -\left(\boldsymbol{F}_D + \Gamma \boldsymbol{v}_i\right), & k = g, \\ \boldsymbol{F}_D + \Gamma \boldsymbol{v}_i, & k = l, s, \end{cases}$$

where the source term $\boldsymbol{F}_D$ is the interfacial momentum exchange between the phases and the quantity $\boldsymbol{v}_i$ is an interfacial velocity.

The interfacial energy transfer for each phases is defined as

$$\sigma_k^Q = \begin{cases} -\left(\boldsymbol{F}_D \cdot \boldsymbol{v}_i + Q + \Gamma(e_i + \dfrac{|\boldsymbol{v}_i|^2}{2})\right), & k = g, \\ \boldsymbol{F}_D \cdot \boldsymbol{v}_i + Q + \Gamma(e_i + \dfrac{|\boldsymbol{v}_i|^2}{2}), & k = l, s, \end{cases}$$

where the source term Q is the interfacial energy exchange between the phases and the quantity e_i is the internal energy.

The density component for each phases is expressed as

$$\rho_k = \begin{cases} \varepsilon_g \cdot \rho_{gas}, & k = g, \\ (1 - \varepsilon_g) \cdot \rho_{liquid}, & k = l, \\ (1 - \varepsilon_g) \cdot \rho_{solid}, & k = s, \end{cases}$$

where ε_g is the gas hold up.

The total energy E_k is expressed as

$$E_k = \rho_k e_k + \rho_k \frac{|\boldsymbol{v}_k|^2}{2}, \quad k = g, l, s,$$

where e_k is the internal energy, such that

$$e_k = c_{vk} T_k, \quad k = g, l, s,$$

where c_{vk} is the specific heat at a constant volume and T_k is the temperature for each $k = g, l, s$.

The gas pressure p_g is computed according to the equation of state for an ideal gas

$$p_g = (\gamma - 1)\rho_g e_g, \tag{2}$$

where e_g is an internal gas energy and γ stands for the specific heat ratio.

In the case of an adiabatic compressible fluid flow without force term the nonlinear system (1) can be written in the form

$$\frac{\partial \boldsymbol{U}}{\partial t} + \sum_{j=1}^{n} \frac{\partial \boldsymbol{F}_j(\boldsymbol{U})}{\partial x_j} = \boldsymbol{0}. \tag{3}$$

Here, $\boldsymbol{F}_j = (F_{j1}, ..., F_{jm})^T : D \to R^m, j = 1, ..., n$ $(m, n \in N)$, is the inviscid Euler flux, which is supposed to be a continuously differentiable function and $D \in R^m$ is an open set. We consider (3) in a space-time cylinder $Q_I = \Omega \times (0, I)$, where $\Omega \in R^n$ is a domain occupied by a gas and $I > 0$.

System (3) is to be equipped with the initial conditions

$$\boldsymbol{U}(\boldsymbol{x}, 0) = \boldsymbol{U}^0(\boldsymbol{x}), \quad \boldsymbol{x} \in \Omega, \tag{4}$$

where $\boldsymbol{U}^0$ is a given vector-valued function.

Moreover, the boundary conditions are given by

$$\boldsymbol{B}(\boldsymbol{U}) = \boldsymbol{0}, \quad \text{on} \quad \partial\Omega \times (0, I), \tag{5}$$

where $\boldsymbol{B}$ is a suitable boundary operator.

The choise of appropriate boundary conditions represents an important problem in the numerical simulation of fluid flow. Boundary conditions have to reflect physical behaviour of the flow on the boundary of the domain occupied by the fluid, but it must correspond to the mathematical character of the solved equations. There are several approaches to the formulation of the boundary conditions, depending on the problem and the geometry of the domain Ω. We write $\partial\Omega = \Gamma_{\mathrm{I}} \cup \Gamma_{\mathrm{O}} \cup \Gamma_{\mathrm{w}}$, where Γ_{I} represents the inlet through which the gas enters the domain Ω, Γ_{O} is the outlet through which the gas should leave Ω and Γ_{W} represents impermeable fixed walls.

Assuming that $\boldsymbol{U} \in C^1(Q_I)^m$, then the system of conservation laws (3) can be written as a quasilinear system of the type

$$A_0(\boldsymbol{U})\frac{\partial \boldsymbol{U}}{\partial t} + \sum_{j=1}^{n} A_j(\boldsymbol{U})\frac{\partial \boldsymbol{U}}{\partial x_j} = 0 \tag{6}$$

with $m \times m$ matrices $A_j(\boldsymbol{U}), j = 0, ..., n$, which depend on the unknown function $\boldsymbol{U}$ in a generally nonlinear way.

Here,

$$\boldsymbol{A}(\boldsymbol{U}) = \frac{\partial \boldsymbol{F}(\boldsymbol{U})}{\partial \boldsymbol{U}} \tag{7}$$

is the Jacobian matrix.

It is well known fact that even the simplest equations of the type (3) exhibit such nonlinear phenomena as nonexistence of global smooth solutions on a massive set of initial and boundary data.

III. Discretization

In fluid dynamics, typically convection-diffusion problems with small or even vanishing diffusion occur. This means that these problems are either singularly perturbed parabolic or hyperbolic.

For a singularly perturbed and hyperbolic equation the standard application of the Galerkin Finite Element Method gives rise to the Gibbs phenomenon, manifested by spurious oscillations in the numerical solution [5]. Therefore, we use two numerical approaches for solving the system. The first numerical approach is the streamline upwind Petrov-Galerkin method (SUPG), i.e. a diffusion term acting only in the direction of the streamlines is added. Second approach is the discontinous Galerkin method (DGM), which uses ideas of the finite element and finite volume methods and provides robust numerical processes and accurate solutions [6]. Moreover, a special treatment of boundary conditions in inviscid convective terms is considered.

A. Space Semidiscretizaton by SUPG

To formulate the SUPG approach, we assume that there exists an exact solution of the problem (3)–(5) and introduce a weak formulation. We multiply the equation (3) by any test function $\boldsymbol{\varphi} \in \boldsymbol{H}^1(\Omega)$, then integrate over Ω and apply Green's theorem and we obtain the relation

$$\int_\Omega \frac{\partial \boldsymbol{U}}{\partial t} \cdot \boldsymbol{\varphi} \mathrm{d}\boldsymbol{x} - \int_\Omega \boldsymbol{F}(\boldsymbol{U}) \cdot \nabla \boldsymbol{\varphi} \mathrm{d}\boldsymbol{x} + \int_{\partial\Omega} \boldsymbol{F}(\boldsymbol{U})\boldsymbol{n} \cdot \boldsymbol{\varphi} \mathrm{d}\boldsymbol{s} = \boldsymbol{0} \quad \forall \boldsymbol{\varphi} \in \boldsymbol{H}^{\boldsymbol{1}}(\Omega), \forall t \in (0, T), \tag{8}$$

where $\boldsymbol{n}$ is the outer normal vector.

Let us assume that Ω is polygonal bounded domain and $\{\mathcal{T}_h\}_h$ be a family of shape regular meshes of Ω formed by closed quadrilaterial elements e, such that $\overline{\Omega} = \cup_{e\in\mathcal{T}_h}\overline{e}$, $e_i \bigcap e_j = \emptyset$ for $e_i, e_j \in \mathcal{T}_h, i \neq j$. The diameters of the elements e are denoted by h_k. The maximum diameter is $h = max_{e\in\mathcal{T}_h} h_k$.

We introduce a finite element space of vector-valued continuous piecewise polynomial functions $\boldsymbol{S_h} = (S_h)^m$, where

$$S_h = \{v \in C(\Omega); v|_e \in P_p(e), \forall e \in \mathcal{T}_h\},$$

where $P_p(e)$ denotes the set of all polynomials on $e \in \mathcal{T}_h$ of degree p.

To approximate the solution $\boldsymbol{U}$ of (8) we solve the problem in the finite dimensional space $\boldsymbol{S_h} = (S_h)^m$ and we obtain:

$$\int_\Omega \frac{\partial \boldsymbol{U}_h}{\partial t}\cdot\boldsymbol{\varphi}_h \mathrm{d}\boldsymbol{x} - \int_\Omega \boldsymbol{F}(\boldsymbol{U}_h)\cdot\nabla\boldsymbol{\varphi}_h \mathrm{d}\boldsymbol{x} + \int_{\partial\Omega} \boldsymbol{F}(\boldsymbol{U}_h)\boldsymbol{n}\cdot\boldsymbol{\varphi}_h \mathrm{d}\boldsymbol{s} = \boldsymbol{0}, \quad \forall\boldsymbol{\varphi}_h \in \boldsymbol{H^1}(\Omega), \forall t \in (0,T). \tag{9}$$

Then we replace the test function $\boldsymbol{\varphi}_h$ by $\boldsymbol{\varphi}_h + \delta_e \boldsymbol{A}(\boldsymbol{U}_h)$, where $\boldsymbol{A}(\boldsymbol{U}_h)$ is defined by (7) and δ_e is the SUPG stabilization parameter. Then the stabilized Galerkin semidiscretizaton in space reads as:

Find $\boldsymbol{U}_h \in C^1([0,T];\boldsymbol{S_h})$ with $\boldsymbol{U_h}(0) = \boldsymbol{U_h}^0$ such that:

$$\int_\Omega \frac{\partial \boldsymbol{U_h}}{\partial t}\cdot\boldsymbol{\varphi_h} \mathrm{d}\boldsymbol{x} - \int_\Omega \boldsymbol{F}(\boldsymbol{U_h})\cdot\nabla\boldsymbol{\varphi}_h \mathrm{d}\boldsymbol{x} + \int_{\partial\Omega} \boldsymbol{N}(\boldsymbol{U}_h^+, \boldsymbol{U}_h^-, \boldsymbol{n})\cdot\boldsymbol{\varphi_h^+} \mathrm{d}\boldsymbol{s} + SUPG(\boldsymbol{U}_h, \boldsymbol{\varphi}_h) + SHOCK(\boldsymbol{U}_h, \boldsymbol{\varphi}_h) = \boldsymbol{0}, \quad \forall\boldsymbol{\varphi}_h \in \boldsymbol{S}_h, \forall t \in (0,T), \tag{10}$$

where $\boldsymbol{\varphi}_h^+$ is the outer trace of a function $\boldsymbol{\varphi}_h$, $\boldsymbol{U}_h^+$ is the interior trace of a function $\boldsymbol{U}_h$, and $\boldsymbol{U}_h^-$ is the outer trace.

The fourth term $SUPG(\boldsymbol{U}_h, \boldsymbol{\varphi}_h)$ of (10) is the streamline diffusion term. This stabilization term is defined by

$$\sum_{e\in\mathcal{T}_h}\int_e \delta_e\left(\frac{\partial \boldsymbol{U}_h}{\partial t} + \boldsymbol{A}(\boldsymbol{U}_h)\cdot\nabla\boldsymbol{U}_h\right)\left(\boldsymbol{A}(\boldsymbol{U}_h)\cdot\nabla\boldsymbol{\varphi}_h\right)\mathrm{d}\boldsymbol{x},$$

where δ_e is the stabilization parameter and $\boldsymbol{A}(\boldsymbol{U}_h)$ is defined by (7). As follows from numerical experiments, the numerical solution obtain discontinuities or steep gradients of the exact solution in a thin numerical layer and within this layer the approximate solution may exhibit overshoots or undershoots. Therefore, we add the fifth term the shock capturing term in (10):

$$\sum_{e\in\mathcal{T}_h}\int_e \eta_e\cdot\nabla\boldsymbol{U}_h\cdot\nabla\boldsymbol{\varphi}_h \mathrm{d}\boldsymbol{x},$$

where η_e is a shock-capturing parameter.

In addition, since the numerical solution $\boldsymbol{U}_h$ is discontinous between element interfaces, we have to replace the flux $\boldsymbol{F}(\boldsymbol{U}_h)\boldsymbol{n}$ by a numerical flux function $\boldsymbol{N}(\boldsymbol{U}_h^+, \boldsymbol{U}_h^-, \boldsymbol{n})$. As numerical flux function we choose the Lax-Friedrichs flux, which is defined as follows:

$$\boldsymbol{N}(\boldsymbol{U}_h^+, \boldsymbol{U}_h^-, \boldsymbol{n}) = \frac{\boldsymbol{F}(\boldsymbol{U}_h^+)\cdot\boldsymbol{n} + \boldsymbol{F}(\boldsymbol{U}_h^-)\cdot\boldsymbol{n}}{2} + \frac{\alpha}{2}(\boldsymbol{U}_h^+ - \boldsymbol{U}_h^-), \tag{11}$$

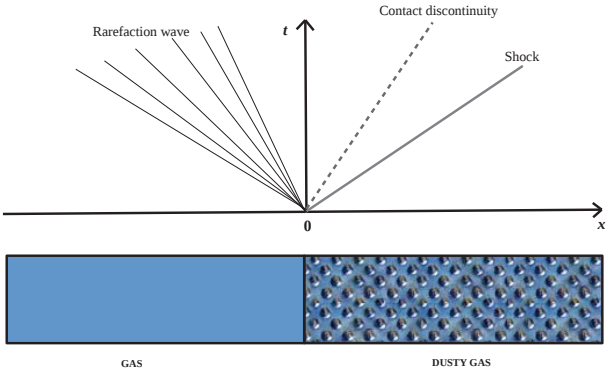

Fig. 1 Schematic diagram of flow in a dusty gas shock tube after diaphragm rupture

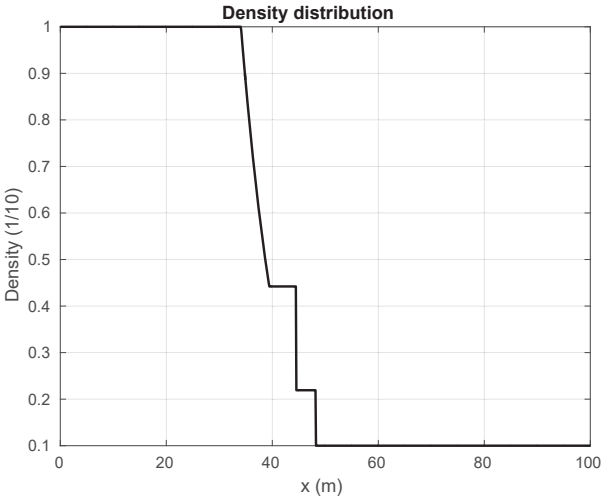

Fig. 2 Exact solution of the pure gas shock tube problem

where $\boldsymbol{n}$ is the outer normal vector, α is fixed number or mesh depend value.

B. Space Semidiscretizaton by DGM

To formulate the discontinous Galerkin method, we assume that there exists an exact solution of the problem (3)–(5) and introduce a weak formulation. To this end, we multiply (3) by a test function $\boldsymbol{\varphi} \in \boldsymbol{H}^1(\Omega, \mathcal{T}_h)$, where $\boldsymbol{H}^1(\Omega, \mathcal{T}_h)$ is the broken Sobolev space over the mesh $\mathcal{T}_h$. Then integrate over any element $e \in \mathcal{T}_h$, apply Green's theorem and sum over all $e \in \mathcal{T}_h$. Then we get

$$\sum_{e\in\mathcal{T}_h}\int_e \frac{\partial \boldsymbol{U}}{\partial t}\cdot\boldsymbol{\varphi}\mathrm{d}\boldsymbol{x} - \sum_{e\in\mathcal{T}_h}\int_e \boldsymbol{F}(\boldsymbol{U})\cdot\nabla\boldsymbol{\varphi}\mathrm{d}\boldsymbol{x} + \sum_{e\in\mathcal{T}_h}\int_{\partial e} \boldsymbol{F}(\boldsymbol{U})\boldsymbol{n}\cdot\boldsymbol{\varphi}\mathrm{d}\boldsymbol{s} = \boldsymbol{0}, \forall\boldsymbol{\varphi} \in \boldsymbol{H^1}(\Omega, \mathcal{T}_h), \forall t \in (0,T), \tag{12}$$

where $\boldsymbol{n} = (n_1, ..., n_m)$ denotes the outer unit normal to the boundary of $e \in \mathcal{T}_h$. We rewrite the surface integrals in (12) over ∂e according to the type of faces $\Gamma \in \mathcal{T}_h$. Then the

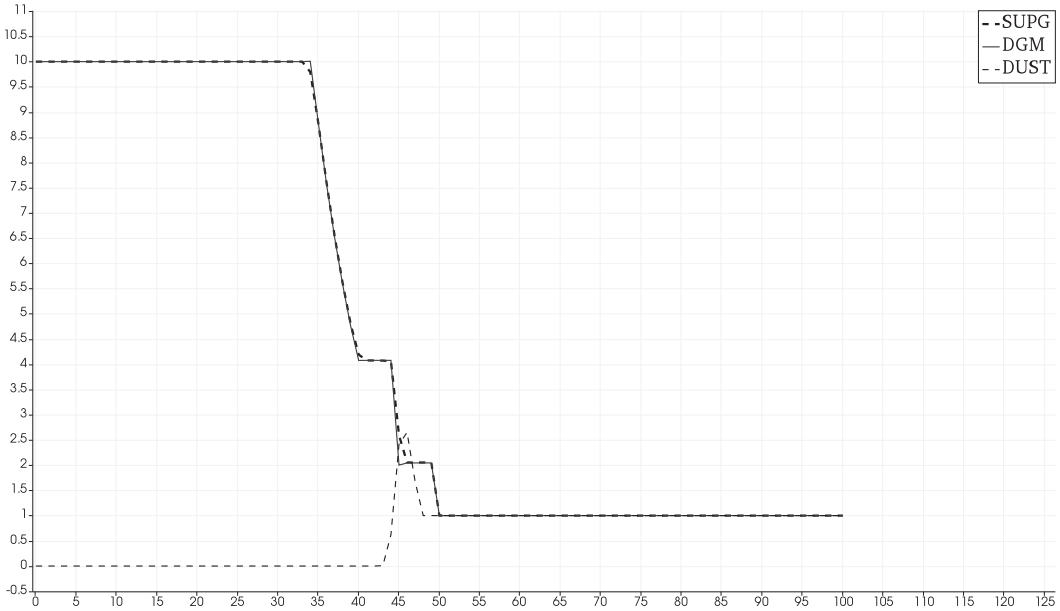

Fig. 3 Density distributions of the pure gas and dust at time $t = 5$

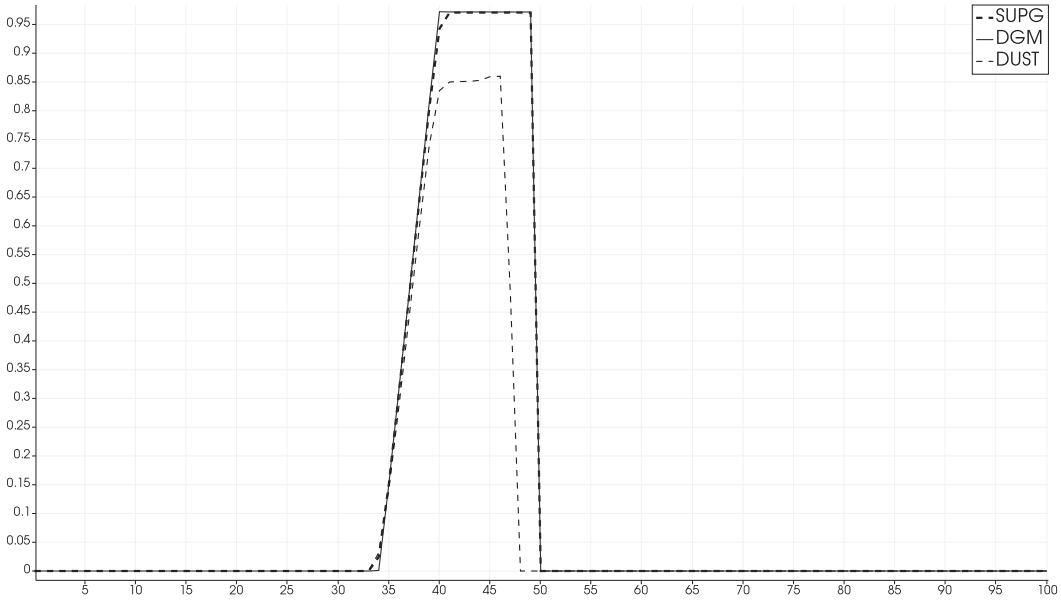

Fig. 4 Velocity distributions of the pure gas and dust at time $t = 5$

discontinous Galerkin weak form reads as following

$$\sum_{e\in\mathcal{T}_h}\int_e \frac{\partial \boldsymbol{U}}{\partial t}\cdot\boldsymbol{\varphi}\mathrm{d}\boldsymbol{x} - \sum_{e\in\mathcal{T}_h}\int_e \boldsymbol{F}(\boldsymbol{U})\cdot\nabla\boldsymbol{\varphi}\mathrm{d}\boldsymbol{x} + \sum_{\Gamma\in\Gamma^I}\int_\Gamma \boldsymbol{F}(\boldsymbol{U})\boldsymbol{n}\cdot[\boldsymbol{\varphi}]\mathrm{d}\boldsymbol{s} + \sum_{\Gamma\in\Gamma^B}\int_\Gamma \boldsymbol{F}(\boldsymbol{U})\boldsymbol{n}\cdot\boldsymbol{\varphi}\mathrm{d}\boldsymbol{s} = \boldsymbol{0} \quad \forall\boldsymbol{\varphi}\in\boldsymbol{H}^1(\Omega,\mathcal{T}_h),\forall t\in(0,T), \tag{13}$$

where Γ^I is an inner face and Γ^B is the boundary face and the jump is defined as $[\boldsymbol{\varphi}] = \boldsymbol{\varphi}^+ - \boldsymbol{\varphi}^-$.
The domain Ω, the mesh $\mathcal{T}_h$ and the quadrilaterial elements e are assumed as before in section A.

The finite element space of vector-valued discontinuous piecewise polynomial functions is defined as $\boldsymbol{V_h} = (V_h)^m$ with

$$V_h = \{v \in L^2(\Omega); v|_e \in P_p(e), \forall e \in \mathcal{T}_h\}.$$

To approximate the solution $\boldsymbol{U}$ of (13) we solve the problem in the finite dimensional space $\boldsymbol{V_h} = (V_h)^m$ and replace the flux $\boldsymbol{F}(\boldsymbol{U}_h)\boldsymbol{n}$ on the boundary by the numerical flux function $\boldsymbol{N}(\boldsymbol{U}_h^+, \boldsymbol{U}_h^-, \boldsymbol{n})$ which is defined in (11). Then the discontinous Galerkin semidiscretizaton in space reads as follows.

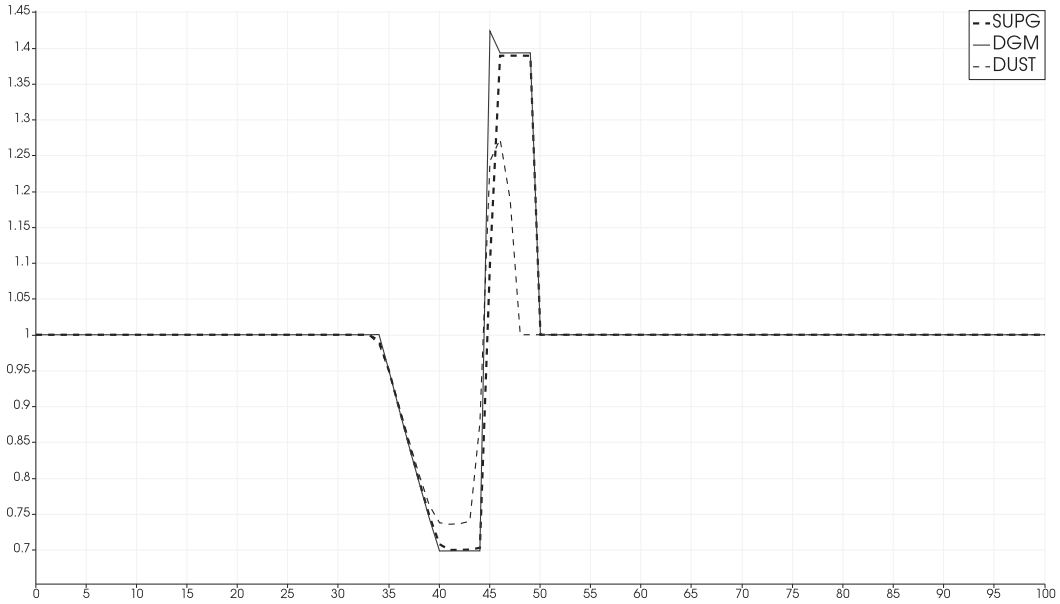

Fig. 5 Temperature distributions of the pure gas and dust at time $t = 5$

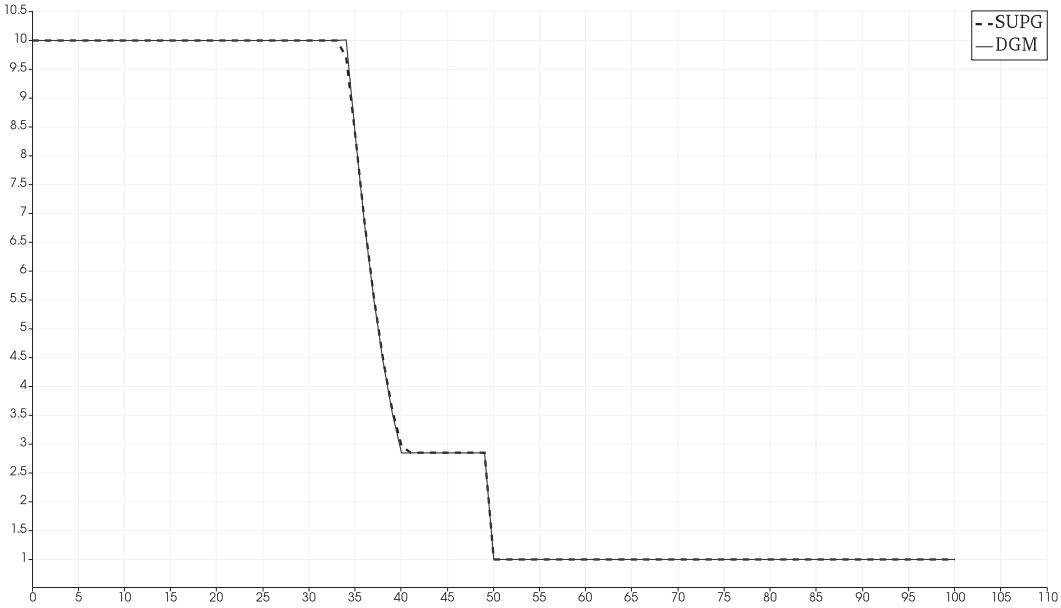

Fig. 6 Pressure distributions of the gas at time $t = 5$

Find $\boldsymbol{U}_h \in C^1([0,T];\boldsymbol{V}_h)$ with $\boldsymbol{U}_h(0) = \boldsymbol{U_h}^0$ such that:

$$\begin{aligned}\sum_{e\in\mathcal{T}_h}\int_e \frac{\partial \boldsymbol{U}_h}{\partial t}\cdot\boldsymbol{\varphi}_h \mathrm{d}\boldsymbol{x} - \sum_{e\in\mathcal{T}_h}\int_e \boldsymbol{F}(\boldsymbol{U}_h)\cdot\nabla\boldsymbol{\varphi}_h \mathrm{d}\boldsymbol{x} \\ + \sum_{\Gamma\in\Gamma_h^I}\int_\Gamma \boldsymbol{N}(\boldsymbol{U}_h^+,\boldsymbol{U}_h^-,\boldsymbol{n})\cdot[\boldsymbol{\varphi}_h]\mathrm{d}\boldsymbol{s} \\ + \sum_{\Gamma\in\Gamma_h^B}\int_\Gamma \boldsymbol{N}(\boldsymbol{U}_h^+,\boldsymbol{U}_h^-,\boldsymbol{n})\cdot\boldsymbol{\varphi}_h \mathrm{d}\boldsymbol{s} = \boldsymbol{0}, \\ \forall\boldsymbol{\varphi}_h\in\boldsymbol{V}_h, \forall t\in(0,T).\end{aligned} \tag{14}$$

C. Time Discretization Using Crank-Nicolson Method

Let $0 = t_0 < t_1 < t_2 ... < t_N = T$ be a subdivision of $I = (0,T)$ with time intervals $I_n = (t_{n-1}, t_n]$ and time steps $k_n = t_n - t_{n-1}$ for $n = 1, ..., N$ and $k = max_{1\le n\le N} k_n$.

We use the notation $\boldsymbol{U}_h^n$ for the approximation of $\boldsymbol{U}_h(t_n)$.

Then, we have the following fully discrete scheme for the SUPG based approach.

Find $\boldsymbol{U}_h^n \in \boldsymbol{S}_h$ with $\boldsymbol{U}_h(0) = \boldsymbol{U_h}^0$ such that:

$$\int_\Omega \frac{\boldsymbol{U}_h^{n+1} - \boldsymbol{U}_h^n}{k} \cdot \boldsymbol{\varphi}_h \mathrm{d}\boldsymbol{x} - \int_\Omega \boldsymbol{F}(\overline{\boldsymbol{U}}_h) \cdot \nabla \boldsymbol{\varphi}_h \mathrm{d}\boldsymbol{x} + \int_\Gamma \boldsymbol{N}(\overline{\boldsymbol{U}}_h^+, \overline{\boldsymbol{U}}_h^-, \boldsymbol{n}) \cdot \boldsymbol{\varphi}_h^+ \mathrm{d}\boldsymbol{s} + SUPG(\overline{\boldsymbol{U}}_h, \boldsymbol{\varphi}_h) + SHOCK(\overline{\boldsymbol{U}}_h, \boldsymbol{\varphi}_h) = \boldsymbol{0}, \quad \forall \boldsymbol{\varphi}_h \in \boldsymbol{S}_h. \tag{15}$$

Similarly we have the following fully discrete scheme for the DGM:

Find $\boldsymbol{U}_h^n \in \boldsymbol{V}_h$ with $\boldsymbol{U}_h(0) = \boldsymbol{U_h}^0$ such that

$$\sum_{e \in \mathcal{T}_h} \int_e \frac{\boldsymbol{U}_h^{n+1} - \boldsymbol{U}_h^n}{k} \cdot \boldsymbol{\varphi}_h \mathrm{d}\boldsymbol{x} - \sum_{e \in \mathcal{T}_h} \int_e \boldsymbol{F}(\overline{\boldsymbol{U}}_h) \cdot \nabla \boldsymbol{\varphi}_h \mathrm{d}\boldsymbol{x} + \sum_{\Gamma \in \mathcal{T}_h^I} \int_\Gamma \boldsymbol{N}(\overline{\boldsymbol{U}}_h^+, \overline{\boldsymbol{U}}_h^-, \boldsymbol{n}) \cdot [\boldsymbol{\varphi}_h] \mathrm{d}\boldsymbol{s} + \sum_{\Gamma \in \mathcal{T}_h^B} \int_\Gamma \boldsymbol{N}(\overline{\boldsymbol{U}}_h^+, \overline{\boldsymbol{U}}_h^-, \boldsymbol{n}) \cdot \boldsymbol{\varphi}_h \mathrm{d}\boldsymbol{s} = \boldsymbol{0}, \quad \forall \boldsymbol{\varphi}_h \in \boldsymbol{V}_h. \tag{16}$$

In fully discrete schemes (14) and (15) we use the abbreviation

$$\overline{\boldsymbol{U}}_h = \frac{\boldsymbol{U}_h^{n+1} + \boldsymbol{U}_h^n}{2}.$$

In algebraic form the problems (15) and (16) represent a nonlinear system of equations, that are solved by a Newton iteration.

D. Numerical Test Problem

We consider the classical problem of the shock tube problem [7], where the driver contains high-pressure gas and the channel contains a dusty gas, which is divided initially by a membrane into two sections, pure gas and the dusty gas. The gas has a higher density and pressure in one half and zero velocity everywhere. The structure of the solution of this shock tube problem involves a rarefaction wave in a left half–plane, contact discontinuity, and the shock wave in a right half–plane, as shown in Fig. 1. The exact solution for the density profile of the pure gas shock tube problem at time $t = 5$ is displayed in Fig. 2.

In order to formulate the motion of the mixture, we need to make some assumptions. The gas is assumed to be perfect and its viscosity and a heat conductivity are neglected except for the interaction with the particles. The particles are assumed to be spheres of an uniform size and their number is so large that the flow may be treated as a continuum. The volume occupied by the particles is neglected.

The described shock tube problem can be modelled by the hyperbolic two–phase flow with nonequilibrium flow conditions, which is based on the two–fluid model.

Gas phase:

$$\begin{aligned} \frac{\partial(\rho_g)}{\partial t} + \bigtriangledown \cdot (\rho_g \boldsymbol{v}_g) &= 0, \\ \frac{\partial(\rho_g \boldsymbol{v}_g)}{\partial t} + \bigtriangledown \cdot (\rho_g \boldsymbol{v}_g \otimes \boldsymbol{v}_g) + \bigtriangledown p &= -\boldsymbol{F}_D, \\ \frac{\partial(E_g)}{\partial t} + \bigtriangledown \cdot ((E_g + p)\boldsymbol{v}_g) &= -\boldsymbol{F}_D \cdot \boldsymbol{v}_i - Q. \end{aligned} \tag{17}$$

Solid phase (dispersed particles):

$$\begin{aligned} \frac{\partial(\rho_s)}{\partial t} + \bigtriangledown \cdot (\rho_s \boldsymbol{v}_s) &= 0, \\ \frac{\partial(\rho_s \boldsymbol{v}_s)}{\partial t} + \bigtriangledown \cdot (\rho_s \boldsymbol{v}_s \otimes \boldsymbol{v}_s) &= \boldsymbol{F}_D, \\ \frac{\partial(E_s)}{\partial t} + \bigtriangledown \cdot (E_s \boldsymbol{v}_s) &= \boldsymbol{F}_D \cdot \boldsymbol{v}_i + Q. \end{aligned} \tag{18}$$

Here, the source terms $\boldsymbol{F}_D$, Q are the drag force and energy exchange between the phases, respectively.

The Drag force source term is defined:

$$\boldsymbol{F}_D = \frac{3}{4} \cdot \frac{\rho_g \cdot \rho_s}{d_s \cdot \rho_{solid}} \cdot C_d \cdot |\boldsymbol{u}_g - \boldsymbol{u}_s| \cdot (\boldsymbol{u}_g - \boldsymbol{u}_s),$$

where, d_s is a particle diameter and C_d is a dimensionless drag coefficient. The drag coefficient is defined [7]:

$$C_d = 112 \cdot Re^{-0.98}.$$

Reynolds number Re is calculated as:

$$Re = \frac{\rho_g \cdot d_s}{\mu_g} \cdot |\boldsymbol{u}_g - \boldsymbol{u}_s|.$$

The temperature dependence of the dynamic viscosity of clorine is obtained according to (Sutherland's formula):

$$\mu_g = 17.17 \cdot 10^{-6} \cdot \frac{(110 + 273)}{(110 + T_g)} \cdot \left(\frac{T_g}{273}\right)^{1.5}.$$

The interface heat transfer source term is defined as:

$$Q = 6 \cdot \frac{\rho_s \cdot \mu_g \cdot c_{pg}}{d_s^2 \cdot \rho_{solid}} \cdot \frac{Nu}{Pr} \cdot (T_g - T_s),$$

where c_{pg} is the specific heat of the gas at constant pressure.

Prandtl number is assumed to be constant

$$Pr = \frac{\mu_g \cdot c_{pg}}{k} = 0.75,$$

where, k is thermal conductivity.

The Nusselt number is defined:

$$Nu = 2.0 + 0.6 \cdot Pr^{1/3} \cdot Re^{1/2}.$$

The equation of state is prescribed in (2).

The system of equations (17)–(18) equipped with initial and boundary conditions.

The jump in the initial data only occurs in the x direction. We solve this problem by two different numerical methods, the DGM and the SUPG approach. We consider the 2D dusty-gas shock tube problem (17)–(18) in the time-space cylinder

$$Q_T = \Omega \times [0, T), \quad T = 5, \quad \Omega = (0, 100) \times (0, 0.1).$$

The initial conditions are given for the gas phase by

$$\left(\rho_g^0, \boldsymbol{v}_g^0, T_g^0\right) = \begin{cases} (10, \quad 0.0, \quad 0.0, \quad 1.0)^T, & x \leq 40, \\ (1.0, \quad 0.0, \quad 0.0, \quad 1.0)^T, & x > 40, \end{cases}$$

and for the solid phase by

$$\left(\rho_s^0, \boldsymbol{v}_s^0, T_s^0\right) = \begin{cases} \left(10^{-4}, \quad 0.0, \quad 0.0, \quad 1.0\right)^T, & x \leq 40, \\ (1.0, \quad 0.0, \quad 0.0, \quad 1.0)^T, & x > 40. \end{cases}$$

The inflow or outflow and the wall impermeable boundary conditions are applied.

The parameter values are defined as in [8]:

$\rho_{\text{solid}} = 2500$ [kg/m^3], $\gamma = 1.4$, $c_{\text{pg}} = 766$ [J/kgK],

$\mid \boldsymbol{u}_{\text{slip}} \mid = 1$ [m/s], $d_{\text{d}} = 27 \cdot 10^{-5}$ [m].

E. Validation: Cross Section Graphics over x Direction

Two numerical results of the DGM and the SUPG approach for the density, the velocity, the temperature and the pressure distributions are shown in Figs. 3-6.

To time $t = 5$ we compare the density, velocity, temperature and pressure distributions computed by the SUPG approach with the DGM. We see that in Fig. 3, Figs. 4 and 6 the approximate solutions obtained by using the DGM for the density, the velocity and the pressure profiles are smoother and exhibit an inherent stability at discontinuities. But as we see in Fig. 5 the approximate solution by the DGM of the temperature profile has nonphysical oscilations in the neighbourhood of the contact discontinuities.

IV. Conclusion

In this paper we considered the mathematical model for the two phase gas–solid flow and discussed two numerical methods: the SUPG approach and the DGM. By using the DGM the approximated solutions present the Gibbs phenomenon propagating at the contact discontinuity. These phenomena do not occur in low Mach number regimes, when the exact solution is regular. But in high–speed flows these phenomena give instabilities in the approximate solution.
A future work plan will involve applications of the DGM with stabilization, based on the concept of artificial viscosity applied locally on the basis of a suitable jump indicator.

Acknowledgment

The authors would like to thank the financial support provided by German Academic Exchange Service (DAAD).

References

[1] A. A. Ignatev, *The assessment of the reasons for the imbalance volumes of gas in the system of provider-consumer[in Russian]*, Natural gas industry. Russian, 2010.
[2] A. Drew and S. Passman, *Theory of Multi-component Fluids*, Springer verlag Inc., New York, 1998.
[3] M. Ishii, *Thermo-Fluid Dynamic Theory of Two-Phase Flow*, Eyrolles, Paris, 1975.
[4] H. Städke, *Gasdynamic Aspects of Two-Phase Flow Hyperbolicity, Wave Propagation Phenomena, and Related Numerical Methods*, https://www.buchhandel.de, 2006.
[5] M. Feistauer, J. Felcman and I. Straškraba *Mathematical and Computational Methods for Compressible Flow*, Clarendon Press, 2003.
[6] V. Dolejši, M. Feistauer *Discontinuous Galerkin Method*, Springer, 2015.
[7] H. Miura and I. I. Glass, *On a dusty gas shock tube*, Institute for Aerospace Studies, University of Toronto, 1981.
[8] M. Sommerfeld, *The unsteadiness of shock waves propagating through gas-particle mixtures*, Experiments in Fluids, 1985.